Supplemental Material of Niwa et al.

Supplemental Materials and Methods

RNAi experiments

Gene knockdown was achieved through RNAi by feeding as described (Timmons and Fire, 1998; Fraser et al., 2000; Kamath et al., 2003). Except for the experiment to obtain the data shown in Figs. 1E and 1F, synchronized populations of L1 larvae were fed bacteria expressing dsRNA corresponding to the target genes. In the experiment shown in Figs. 1E and 1F, synchronized L1 larvae of *mir-48(n4097);mir-84(n4037)* were grown on NGM plates containing *E. coli* OP50 bacterial lawns until 36-hours after hatching at 20ºC. Then, these early L4 animals were put on RNAi plates. In mock RNAi experiments, bacteria carrying a control empty vector were used. The following RNAi vectors from the Julie Ahringer's library (Fraser et al., 2000; Kamath et al., 2003) were used: JA:C42D8.8 for *apl-1*, JA:46C8.6 for *dpy-7*, JA:F13D11.2 for *hbl-1*, JA:Y17G7A.2 for *lin-29*, JA:C12C8.3 for *lin-41* and JA:R31.1 for *sma-1*. A *lin-42* RNAi construct, which targets a region of *F47F6.1a*, was kindly provided by D. Banerjee. To generate another *apl-1* RNAi vector, pRN001, that corresponded to a region of *apl-1* not included in JA:C42D8.8, a PCR fragment of 0.8 kb was amplified from genomic DNA by primers RN160 (5´-GACTCTAGATGACGGTGGGTAAACTAATGATTG-3´) and RN161 (5´-TGACTCGAGCTTGTCAACCTTCTTTCTGTGCTTC-3´) and then digested with *Xho*I and *Xba*I. The digested PCR product was subcloned into plasmid pL4440 (Timmons and Fire, 1998) digested with *Xho*II and *Xba*I. For the a *sel-12* RNAi vector, a PCR

fragment amplified from genomic DNA primers SEL-F-XBA (5´-TCTAGATGCCTTCCACAAGGAGACAACAG-3´) and SEL-R-XHO (5´-CTCGAGACTTGTGTAACAAATGGGGTGATGATC-3´) was subcloned into pCR2.1 (Invitrogen). The insert from the *sel-12*-pCR2.1 plasmid digested by *Xho*I and *Xba*I was then subcloned into pL4440.

We confirmed that *lin-29(RNAi)* adults showed a retarded phenotype and did not produce any alae structure after the L4 molt (100%; *n*=55) as expected, even though *lin-29(RNAi)* did not have any obvious effect on *apl-1::gfp* expression (Fig. 4E). For *apl-1(RNAi)*, we used the JA:C42D8.8 clone to obtain data shown in Figs. 1, 2 and Supplemental S2, whereas the pRN001 construct was used for data shown in Supplemental Fig. S1.

Reverse transcrption (RT)-PCR to verify gene knockdown

Total RNA was extracted from L4 larvae treated with mock RNAi and *apl-1(RNAi)* using the JA:C42D8.8 clone. After the RNA extraction using TRIzol (Invitrogen), genomic DNA was digested by DNA-*free* DNase Treatment and Removal Reagents (Ambion). Single-stranded cDNA was synthesized from total RNA (1 μg for each sample) with oligo(dT) primers and RETROscript (Ambion) according to the manufacture's instructions. The primers APL-5 (5´-GCGACATGAGAAGTTCATTCCA-3´) and APL-3 (5´-CTTTCCAGCTTCATCCTTCCAG-3´) were used to amplify a portion of the *apl-1* transcripts. These primers were chosen such that any potentially remaining genomic DNA contamination would have resulted in larger amplification products. These products would have been easily distinguishable from RT products on agarose gels; however, no

contaminating bands were observed in any sample. The control primers against the *eft-2* housekeeping gene were previously described (Grosshans et al., 2005). Equal volumes of the PCR reactions were analyzed by agarose gel electrophoresis and were quantified by using the Bio-Rad Gel Doc system and Image-J software (Abramoff et al., 2004).

Generating transgenic lines

GFP constructs were generated via single end overlap extension PCR (Boulin et al., 2006). For generating the *apl-1::gfp::unc-54* reporter, a PCR fragment of 1.9 kb containing the *nls-gfp* gene and the 3´UTR from the *unc-54* gene was amplified from the pPD95.70 vector (A. Fire) using the primers GFP70-F (5´-ATGACTGCTCCAAAGAAGAAGCGTAAGG-3´) and GFP2C (Esquela-Kerscher et al., 2005). In parallel, a PCR fragment of 7.0 kb, consisting of the *apl-1* promoter region, was amplified using the primers APL15051 (5´-CCGATCTCGTGAGACTGTTTTTGATG-3´) and APL-B3-70 (5´-CCTTACGCTTCTTCTTTGGAGCAGTCATGGCTGAAAAAATGTCTG-3´) from N2 genomic DNA. Equal amounts of the above-mentioned PCR products were added for primer extension using the primers GFP2C and APL15136 (5´-GAGGAATACCGTGTCTGAACCTTC-3´), resulting in an *apl-1::gfp::unc-54* fusion construct that contains 6997 bp upstream region from the 1st codon (ATG) of *apl-1*. For creating the *apl-1::gfp* construct fused with the *apl-1* 3´UTR (*apl-1::gfp::apl-1*), the 1.9 kb and 7.0 kb PCR fragments described above were mixed for primer extension using the primers APL15136 (5´-GAGGAATACCGTGTCTGAACCTTC-3´) and GFP-R (5´-TTTGTATAGTTCATCCATGCCATG-3´) to obtain a new PCR fragment containing

the *apl-1* promoter conjugated with a *gfp*-coding region without the *unc-54* 3´UTR. In parallel, a PCR fragment containing *apl-1* 3´UTR was amplified using the primers APLUTR1 (5´-CATGGCATGGATGAACTATACAAATAAACCACCAAGACCGTAC-3´) and APLUTR-R2 (5´-CATCATTATTACTAAATGTTTCCTG-3´) from N2 genomic DNA. The PCR products of *apl-1::gfp* and *apl-1* 3´UTR were used for the second PCR reaction with the primer APL15136 and APLUTR-R2, resulting in the *apl-1::gfp::apl-1* reporter.

For both constructs, two independent PCR reactions were combined to ensure that most of the product lacked unwanted mutations. Injection was essentially as described (Jin, 1999; Evans, 2006). Each construct was injected into N2 animals at ~40 ng/µl with *rol-6(su1006)* as a coinjection marker at 80 ng/µl. We used animals carrying integrated *apl-1::gfp* constructs to observe *apl-1* expression for all experiments described in this manuscript. Chromosomal integration of extrachromosomal transgenes was performed using trimethylpsoralen (Sigma-Aldrich) and subsequent UV-irradiation, as essentially described (http://130.15.90.245/tmp_uv_integration.htm). Independent integrated lines from two independent extrachromosomal arrays exhibited comparable expression patterns (Supplemental Fig. S4). *apl-1::gfp::unc-54* integrated line carrying both the *mir-48(n4097)* and *mir-84(n4037)* mutations were genotyped using PCR as described (Abbott et al., 2005).

X-Gal Assay

X-gal staining of animals expressing the *lacZ* gene transcribed under the control of the constitutive, seam cell-specific *col-10* promoter was performed as described (Wightman et al., 1993; Grosshans et al., 2005). The entire 3´ UTR of *apl-1* was amplified from genomic

DNA by PCR using primers RN101 (5´- CCGCGGACCACCAAGACCGTAC -3´) and RN102 (5´- CCATGGCATCATTATTACTAAATGTTTCCTG -3´) and then subcloned into plasmid B29 (Ha et al., 1996) Two independent lines, carrying extrachromosomal arrays, were tested for β-galactosidase expression.

Supplemental References

Abbott, A. L., Alvarez-Saavedra, E., Miska, E. A., Lau, N. C., Bartel, D. P., Horvitz, H. R., Ambros, V., 2005. The *let-7* MicroRNA family members *mir-48*, *mir-84*, and *mir-241* function together to regulate developmental timing in *Caenorhabditis elegans*. Dev. Cell 9**,** 403-414.

Abramoff, M. D., Magelhaes, P. J., Ram, S. J., 2004. Image Processing with ImageJ. Biophotonics International 11**,** 36-42.

Boulin, T., Etcheberger, J. F., Hobert, O., Reporter gene fusions. In: WormBook. The *C. elegans* Research Community (Ed.), 2006, pp. doi/10.1895/wormbook.1891.1106.1891.

Enright, A. J., John, B., Gaul, U., Tuschl, T., Sander, C., Marks, D. S., 2003. MicroRNA targets in *Drosophila*. Genome Biol. 5**,** R1.

Esquela-Kerscher, A., Johnson, S. M., Bai, L., Saito, K., Partridge, J., Reinert, K. L., Slack, F. J., 2005. Post-embryonic expression of *C. elegans* microRNAs belonging to the *lin-4* and *let-7* families in the hypodermis and the reproductive system. Dev. Dyn. 234**,** 868-877.

Evans, T. C., Transformation and microinjection. In: WormBook. The *C. elegans* Research

Community (Ed.), 2006, pp. doi/10.1895/wormbook.1891.1108.1891.

Fraser, A. G., Kamath, R. S., Zipperlen, P., Martinez-Campos, M., Sohrmann, M., Ahringer, J., 2000. Functional genomic analysis of *C. elegans* chromosome I by systematic RNA interference. Nature 408**,** 325-330.

Grosshans, H., Johnson, T., Reinert, K. L., Gerstein, M., Slack, F. J., 2005. The temporal patterning microRNA *let-7* regulates several transcription factors at the larval to adult transition in *C. elegans*. Dev. Cell 8**,** 321-330.

Ha, I., Wightman, B., Ruvkun, G., 1996. A bulged *lin-4*/*lin-14* RNA duplex is sufficient for *Caenorhabditis elegans lin-14* temporal gradient formation. Genes Dev. 10**,** 3041-3050.

Jin, Y., Transformation. In: *C. elegans*: A practical approach. I. A. Hope (Ed.), Oxford University Press, New York, 1999, pp. 69-96.

John, B., Enright, A. J., Aravin, A., Tuschl, T., Sander, C., Marks, D. S., 2004. Human MicroRNA targets. PLoS Biol. 2**,** e363.

Kamath, R. S., Fraser, A. G., Dong, Y., Poulin, G., Durbin, R., Gotta, M., Kanapin, A., Le Bot, N., Moreno, S., Sohrmann, M., Welchman, D. P., Zipperlen, P., Ahringer, J., 2003. Systematic functional analysis of the *Caenorhabditis elegans* genome using RNAi. Nature 421**,** 231-237.

Lall, S., Grun, D., Krek, A., Chen, K., Wang, Y. L., Dewey, C. N., Sood, P., Colombo, T., Bray, N., Macmenamin, P., Kao, H. L., Gunsalus, K. C., Pachter, L., Piano, F., Rajewsky, N., 2006. A genome-wide map of conserved microRNA targets in *C. elegans*. Curr. Biol. 16**,** 460-471.

Lin, S. Y., Johnson, S. M., Abraham, M., Vella, M. C., Pasquinelli, A., Gamberi, C.,

Gottlieb, E., Slack, F. J., 2003. The *C. elegans hunchback* homolog, *hbl-1*, controls temporal patterning and is a probable microRNA target. Dev. Cell 4**,** 639-650.

Timmons, L., Fire, A., 1998. Specific interference by ingested dsRNA. Nature 395**,** 854.

Wightman, B., Ha, I., Ruvkun, G., 1993. Posttranscriptional regulation of the heterochronic gene *lin-14* by *lin-4* mediates temporal pattern formation in *C. elegans*. Cell 75**,** 855-862.

Supplemental Figure Legends

Fig. S1. A second RNA interference (RNAi) construct targeting a different region of the *apl-1* gene also interacts with heterochronic genes. *apl-1* RNAi construct pRN001 was used to obtain data shown in this figure. (A) Percentage of *let-7(n2853)* animals with the bursting vulval phenotype. (B) The molting defect of double mutants of *apl-1* and *hbl-1* at the L4 molt. Each number in parentheses indicates *n* of observed animals in each sample. **p*<0.001 chi-square test.

Fig. S2. *apl-1(RNAi)* does not cause and modify heterochronic phenotypes in wild type and loss-of-function mutants of *hbl-1* and *lin-41*. Effects of feeding bacteria expressing dsRNA corresponding to *apl-1* on wild type animals are described. All data in this figure were obtained using bacteria expressing the JA:C42D8.8 construct from Julie Ahringer's feeding-RNAi library. N2 is wild type. Each number in parentheses indicates *n* of observed seam cells of each sample. (A) *apl-1* RNAi causes a significant, though mild reduction of *apl-1* mRNA level. Quantitative RT-PCR was performed to examine the mRNA level of *apl-1* in *apl-1(RNAi)* animals and control (mock) RNAi L4 animals. Vertical axis indicates the fold-increase of the *apl-1* mRNA expression level normalized by the level of a loading control *eft-2* (±SEM, *N*=4). The level of *apl-1* expression in the mock RNAi animals is represented as 1 on the vertical axis. ***p*<0.01 Student's *t*-test. (B) *apl-1(RNAi)* causes a growth defect in adult stage animals. Each bar represents mean body length with standard error mean (SEM). **p*<0.001 from the Student's *t*-test. (C) Percentage of animals showing alae formation in L4 and adult stages in mock RNAi and *apl-1(RNAi)*. (D) Percentage of

animals showing precocious seam cell fusion at L4 stage in *syIs78* strain, an integrated *ajm-1::gfp* fusion, with mock RNAi and *apl-1(RNAi)*. (E) Percentage of animals showing precocious alae formation at the late L3 stage in *hbl-1* and *lin-41* mutants. (F) Percentage of animals showing adult specific collagen *col-19* expression in the early and mid L4 stages of *maIs105*, an integrated *col-19::gfp* fusion, in the *hbl-1(ve18)* background with mock RNAi and *apl-1* RNAi. While the *hbl-1(ve18)* mutation causes precocious *col-19::gfp* expression in the mid L4 stage, *apl-1(RNAi)* did not alter the timing of this temporal expression pattern.

Fig. S3. *apl-1* is expressed in several types of cells throughout the length of the animals. (A, B) Adult carrying *apl-1::gfp::unc-54* (medial plane of focus). GFP signals were observed in the head and pharynx (a), spermatheca (b), uterus and vulva (c), some cells in tail (d) and ventral neurons (arrowheads). Although this animal also exhibited GFP expression in seam cells (data now shown), the signal was not represented in A because seam cells are lateral and therefore out of focus. (C-E) The overall GFP expression pattern shown in A was almost identical to data from in situ hybridizations. Each panel in C-E was obtained using probes derived from three independent cDNA clones encoding *apl-1*: (C) clone 506h9 (http://nematode.lab.nig.ac.jp/db2/ShowGeneInfo.php?celk=CELK07063); (D) clone 560e1 (http://nematode.lab.nig.ac.jp/db2/ShowGeneInfo.php?celk=CELK01132); and (E) clone 573a2 (http://nematode.lab.nig.ac.jp/db2/ShowGeneInfo.php?celk=CELK00101). In situ data courtesy of Y. Kohara.

Fig. S4. Another *apl-1::gfp::unc-54* integrated line also exhibits a temporal change of GFP

expression in seam cells under the control of heterochronic genes. In this figure, all data were obtained using a different integrated line from the strain represented in Figs. 3, 4 and S3. Strong GFP expression of *apl-1::gfp::unc-54* was observed in seam cells in late (B) but not early (A) L4 stages. Images A and B were taken for the same exposure time and processed identically. Arrows and arrowheads in lower DIC panels point to distal gonad tips and vulvas, respectively. (C) Temporal expression profiles in seam cells of this *apl-1::gfp::unc-54* line in wild type, *hbl-1(RNAi)* or *lin-41(RNAi)* backgrounds. Staging of L4 animals were by relative positions of gonadal tips to vulva: early, mid and late L4 animals were defined as animals showing 0-1/4, 1/4-1/2 and >1/2 gonadal turns, respectively. Overall temporal expression profiles were almost the same as the profile using the original integrated strain shown in Figs. 3 and 4. Each number in parentheses represents *n* of each sample.

Fig. S5. Potential interactions between *apl-1* 3´UTR and miRNAs. Diagram of the *apl-1* 3´UTR showing potential binding sites for the miRNAs. These candidate binding sites have been identified by two bioinformatics programs, miRanda (Enright et al., 2003; John et al., 2004) and PicTar (Lall et al., 2006), and described in WormBase (http://www.wormbase.org/db/seq/gbrowse/wormbase/?name=X:5111600..5118111).
Arrows and arrowheads indicate the sites predicted by miRanda and PicTar, respectively. Potential RNA::RNA duplexes between *apl-1* 3´UTR and the *let-7* family miRNAs, *miR-48* and *miR-265*, are also shown in A-C. Positions of the candidate binding sites in the *apl-1* 3´UTR are indicated by nucleotide numbers in parentheses, which correspond to DNA sequence data deposited in GenBank (accession number: NM_076469). Each colon (:)

indicates G:U Wobble base pair.

Fig. S6. Schematic model for the function of *apl-1* and heterochronic genes in seam cells. Model for the relationship between *apl-1* and heterochronic genes at L4-to-adult transition in wild type (A), *let-7* family mutants (B), and mutants of *hbl-1(lf)*, *lin-41(lf)* and *lin-42(lf)* (C). Positive regulation is denoted by an arrowhead and negative regulation by a perpendicular line. Vertical and horizontal axes of each graph represent a relative level of gene product in seam cells and a developmental time course from L4 to adult stages, respectively.

We propose that the heterochronic pathway temporally regulates *apl-1* expression in seam cells to control proper timing of development and proper molting. In wild type, our data indicate that HBL-1, LIN-41 and LIN-42 repress *apl-1* expression in seam cells in early L4 stages and activate it in the late L4 and adult stages (A). This is consistent with the previous observation that *hbl-1* appears to play both negative and positive roles in regulating adult fates in seam cells (Lin et al., 2003), although the molecular mechanism of this dual function is unknown. In late L4 larvae and adults, the higher levels of *let-7* family miRNAs repress HBL-1, LIN-41 and LIN-42 to modest levels allowing *apl-1* expression and normal seam cell development and L4 molting (A).

This model explains the increased level of *apl-1* in *let-7* family mutants. *let-7* family mutants have increased activities of HBL-1, LIN-41 and LIN-42 in the late L4 and adult stages (B). In late L4 and adult stages, the higher dose of HBL-1, LIN-41 and LIN-42 might induce excessive *apl-1* transcription seen in these seam cells and a defect in seam cell differentiation (B). This model would explain why loss of *apl-1* suppresses the seam

cell defects of *let-7* mutants. In contrast, in early L4 stage *let-7* family mutants, *apl-1* expression in seam cells is still repressed by HBL-1, LIN-41 and LIN-42. Therefore, timing of the *apl-1* expression is not altered. In *hbl-1(lf)*, *lin-41(lf)* and *lin-42(lf)* mutants, *apl-1* expression in seam cells is derepressed in the early L4 stage and is not induced in later development (C). It should be emphasized that *apl-1* expression is not abolished in these mutants in the late L4: we still observe considerable amounts of *apl-1* transcription (Fig. 4E). We hypothesize that this small but consistent amount of *apl-1* in seam cells is enough to perform the molting process at the L4 to adult transition in these mutants, but when *apl-1* is further reduced through RNAi, the animals fail to molt properly. This model therefore explains the synergistic effects of *apl-1(RNAi)* with loss-of-function of *hbl-1*, *lin-41* and *lin-42* in the regulation of the L4 molt.

Supplemental Fig. S1
Niwa et al.

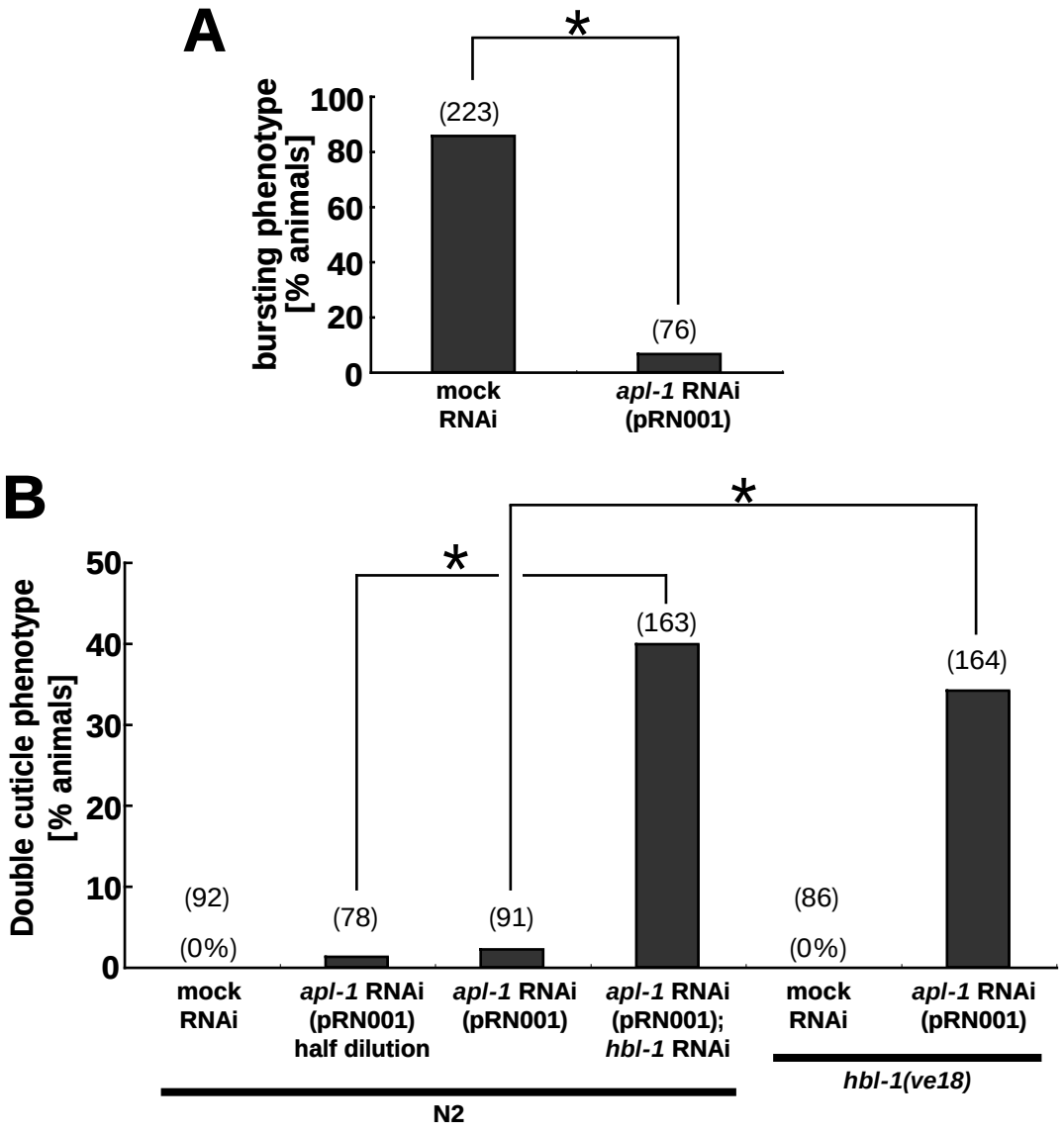

Supplemental Fig. S2
Niwa et al.

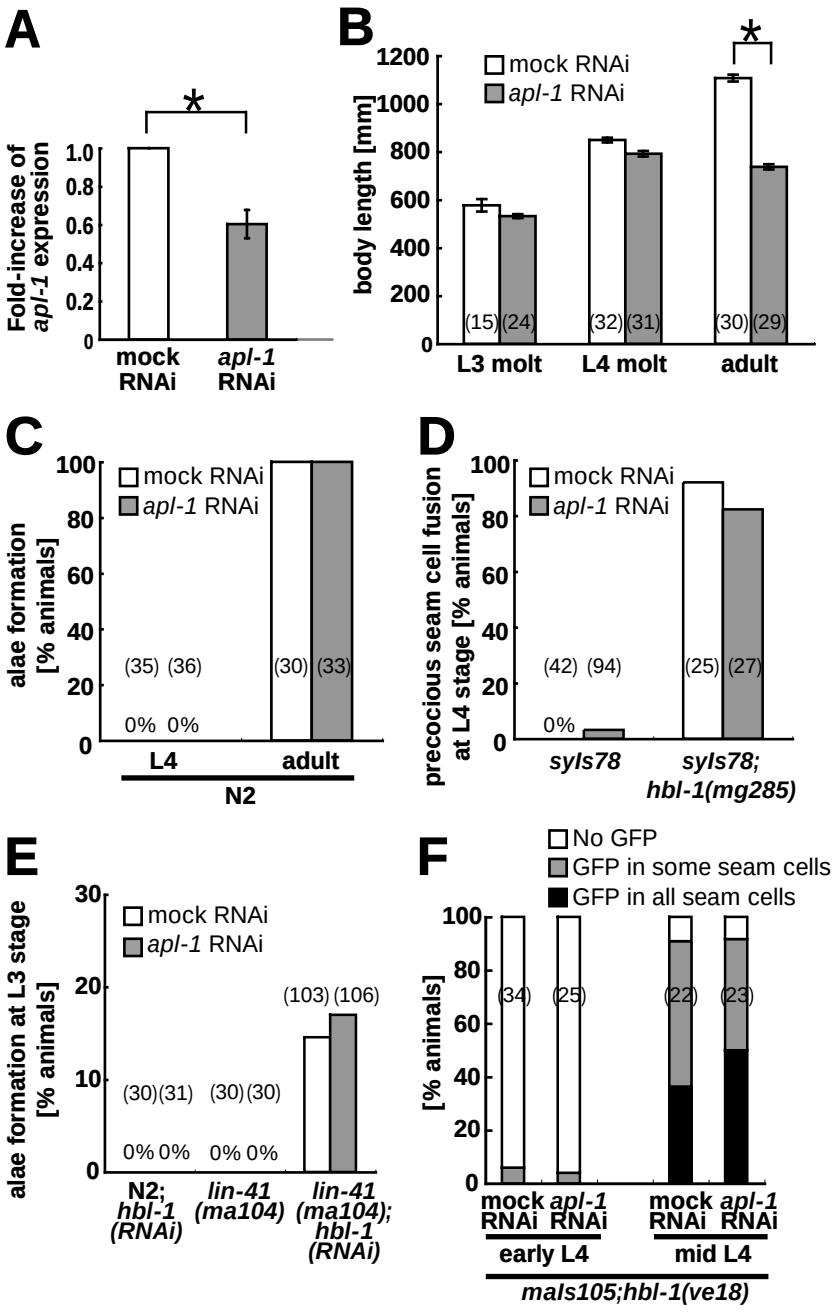

Supplemental Fig. S3
Niwa et al.

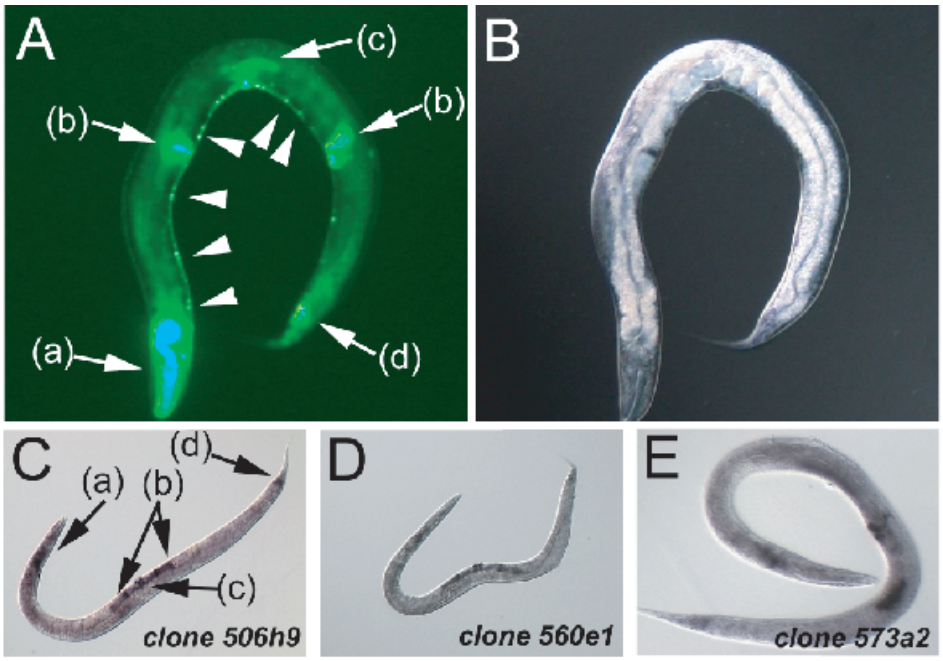

Supplemental Fig. S4
Niwa et al.

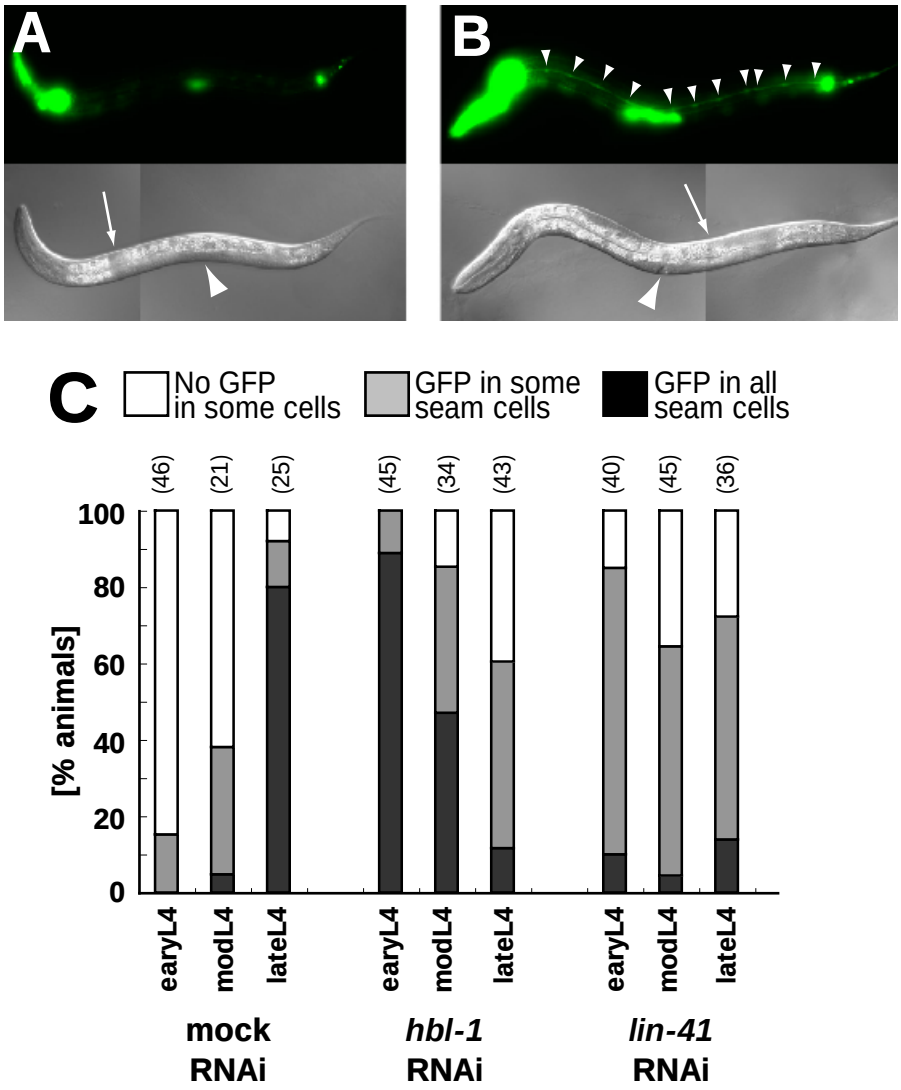

Supplemental Fig. S5
Niwa et al.

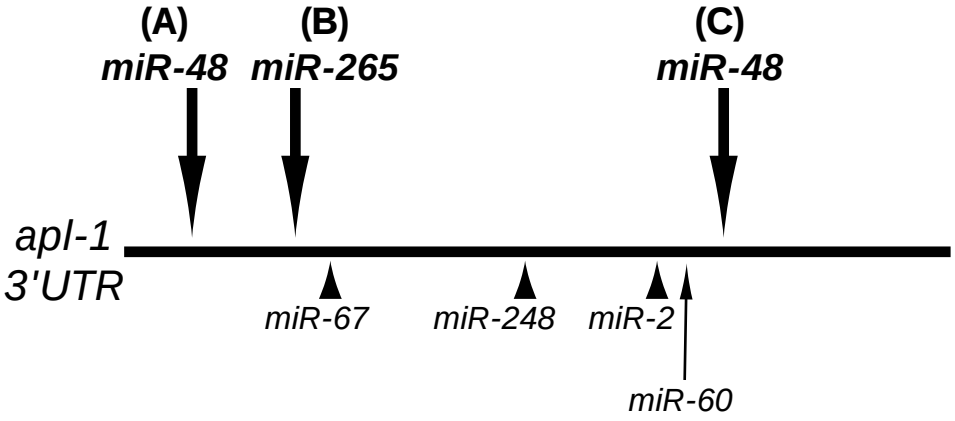

(A)

```
    C      CU
UG AUC AUU CCUAUCUC   apl-1(2118-2136)
GC UAG UGA GGAUGGAG   miR-48
A G  A  CUC
```

(B)

```
C       C
 U CCACCCUCCUCUCUC   apl-1(2198-2215)
 A GGUGGGAGGAGGGAG   miR-265
U U       A     U
```

(C)

```
   G AC U     C       U
UCGU A  U CUACU GUUUCUUC   apl-1(2667-2691)
AGCG U  A GAUGA CGGAGGAG   miR-48
                CU      U
```

Supplemental Fig. S6
Niwa et al.